

# Quantifying the Complexity of Standard Benchmarking Datasets for Long-Term Human Trajectory Prediction

Ronny Hug<sup>†</sup>, Stefan Becker<sup>†</sup>, Wolfgang Hübner<sup>†</sup> and Michael Arens<sup>†</sup>

**Abstract**—Methods to quantify the complexity of trajectory datasets are still a missing piece in benchmarking human trajectory prediction models. In order to gain a better understanding of the complexity of trajectory datasets, an approach for deriving complexity scores from a prototype-based dataset representation is proposed. The dataset representation is obtained by first employing a non-trivial spatial sequence alignment, which enables a following learning vector quantization (LVQ) stage. A large-scale complexity analysis is conducted on several human trajectory prediction benchmarking datasets, followed by a brief discussion on indications for human trajectory prediction and benchmarking.

## I. INTRODUCTION

Creating a not too simple or too hard-to-solve benchmark for human trajectory prediction is still a difficult task. One of the difficulties, is the open question of how the complexity of a given dataset for trajectory prediction can be quantified. As a consequence, current attempts in standardized benchmarking originate from heuristics or experience-based criteria when assembling the data basis. Recent examples are the *TrajNet* challenge [1] or its extension *TrajNet++*, as mentioned in [2].

A common approach for qualitative analysis of data complexity are low-dimensional embeddings for data visualization, like for example *t-SNE* [3] or variations of *PCA* [4]. While such approaches are viable for non-sequential, high-dimensional data, a prototype-based clustering approach seems more viable for sequential data. This is especially true for trajectory datasets, where each dataset can be reduced to a small number of prototypical sub-sequences specifying distinct motion patterns, where each sample can be assumed to be a variation of these prototypes.

Towards this end, an approach for quantifying the relative<sup>1</sup> complexity of a dataset given such a representative set of prototypes is proposed. The approach applies a spatial alignment<sup>2</sup> step followed by vector quantization for clustering aligned samples of the same cardinality, as described in sections III and IV. Regarding previous work, this paper is an extension of [5] and focuses mainly on quantifying dataset complexity. The main contributions are:

- 1) A learning and heuristics-based approach for finding a quantized representation of trajectory datasets.

<sup>†</sup>Fraunhofer IOSB, Ettlingen, Fraunhofer Institute of Optronics, System Technologies and Image Exploitation, 76275 Ettlingen, Germany [firstname.lastname@iosb.fraunhofer.de](mailto:firstname.lastname@iosb.fraunhofer.de)

Fraunhofer IOSB is a member of the Fraunhofer Center for Machine Learning.

<sup>1</sup>Derived complexity scores allow a relative comparison between given datasets

<sup>2</sup>Not to be confused with a temporal sequence alignment

- 2) A first approach for quantifying relative trajectory dataset complexity.
- 3) A large-scale complexity analysis of standard benchmarking datasets for human trajectory prediction.

The evaluation section VI gives a detailed description of the complexity analysis and a ranking of all datasets in comparison. Additionally, implications for the current state of human trajectory prediction and benchmarking, resulting from the analysis, are discussed in section VI-B.

## II. DEFINITIONS AND NOTATION

For convenience, several definitions and notation used throughout the paper are introduced in this section.

- A trajectory  $X$  is defined as an ordered set<sup>3</sup> of points  $\{\mathbf{x}_1, \dots, \mathbf{x}_N\}$ .
- The *length* of a (sub-)trajectory  $X$  always refers to its cardinality  $|X|$ , rather than the spatial distance covered.
- The *distance* between two trajectories  $X$  and  $Y$  of the same length  $|X| = |Y|$  is defined as  $d_{tr}(X, Y) = \sum_{j=1}^{|X|} \|\mathbf{x}_j - \mathbf{y}_j\|_2$ .
- The number of samples, the trajectory length and the number of prototypes are denoted as  $N$ ,  $M$  and  $K$  respectively. For indexing,  $i$ ,  $j$  and  $k$  are used.
- The  $q$ -quantile, with  $q \in [0, 1]$ , of a set of numbers  $\{\cdot\}$  is denoted as  $Q_q(\{\cdot\})$ .

## III. SPATIAL SEQUENCE ALIGNMENT

Given a set of trajectories (*samples*)  $\mathcal{X} = \{X_1, \dots, X_N\}$ , as sequences of  $M$  subsequent points  $X_i = \{\mathbf{x}_1^i, \dots, \mathbf{x}_M^i\}$ , each sample is first normalized by moving it into an arbitrary reference frame and scaling it to unit length:

$$X_i^{norm} = \left\{ \frac{\mathbf{x}_j^i - \bar{\mathbf{x}}}{\mathbf{x}_M^i - \mathbf{x}_1^i} \mid j \in [1, M] \right\}. \quad (1)$$

It has to be noted that this normalization solely serves the purpose of moving all samples into a common value range and therefore it is not a good normalization in terms of pooling similar samples. Then, all samples are aligned relative to a single learned prototype  $\hat{Y} = \{\hat{\mathbf{y}}_1, \hat{\mathbf{y}}_2, \dots, \hat{\mathbf{y}}_M\}$  by using similarity transformations, which are retrieved from a regression model  $\phi : X \rightarrow \{\mathbf{t}, \alpha, s\}$  with translation  $\mathbf{t}$ , rotation angle  $\alpha$  and scale  $s$ .  $\hat{Y}$  and  $\phi$  are learned by

<sup>3</sup>strictly speaking it is not a *true* mathematical set, as it might contain duplicates.

minimizing the mean squared error between each aligned sample  $X_i^\phi = \phi(X_i^{norm})$  and the prototype  $\hat{Y}$

$$\mathcal{L}_{\text{align}}(\phi(X_i^{norm}), \hat{Y}) = \frac{1}{M} \sum_{j=1}^M \|\mathbf{x}_j^i - \hat{\mathbf{y}}_j\|_2^2 \quad (2)$$

using stochastic gradient descent. This is different from linear factor models, where the whole training set has to be considered. With respect to equation 2 and the similarity transformation, the trivial solution that maps all samples onto the zero-vector has to be avoided. A brute force approach to this problem is to enforce a minimum scale for the prototype. These steps result in a minimum variance alignment of all samples with respect to the learned prototype. Further, by learning the prototype and the transformation concurrently, the prototype adapts to the most dominant motion pattern and the normalized data is aligned accordingly.

An exemplary result of this alignment approach is depicted in figure 1. By aligning all samples with a single prototype, aligned samples have a common orientation and form clusters of similar samples.

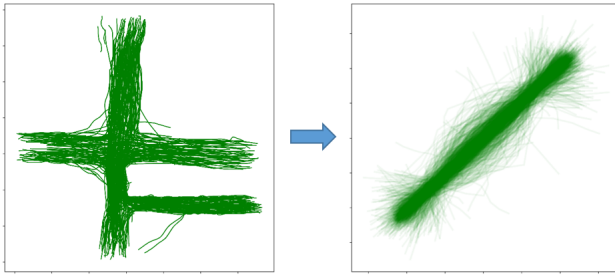


Fig. 1. Example for a resulting alignment (right) of a given dataset (left: *hyang* scene taken from the Stanford Drone Dataset [6]).

#### IV. LEARNING VECTOR QUANTIZATION

Clustering approaches can be applied after the spatial alignment, as it distributes random errors homogeneously over the sequence and exposes clusters of motion patterns. For clustering, a learning vector quantization (LVQ, [7]) approach is employed, which is inspired by [8] and can directly be integrated into a deep learning framework. Here, aligned samples are mapped onto  $K$  prototypes<sup>4</sup>  $\mathcal{Z} = \{Z_1, \dots, Z_K\}$ , with  $Z_k = \{\mathbf{z}_1^k, \dots, \mathbf{z}_M^k\}$ , in quantized space. This results in a concise set of prototypes representing the given dataset. The prototypes are learned by minimizing the mean squared error between the aligned samples  $\mathcal{X}^\phi = \{X_1^\phi, \dots, X_N^\phi\}$  and the respective closest prototype  $Z_{z(i)}$  in quantized space:

$$\mathcal{L} = \underbrace{\frac{1}{N} \sum_{i=1}^N d_{tr}(X_i^\phi, Z_{z(i)})}_{\mathcal{L}_{LVQ}} + \gamma L_{reg}. \quad (3)$$

The index of the closest prototype for a sample  $X_i^\phi$  is determined by

$$z(i) = \arg \min_k d_{tr}(X_i^\phi, Z_k). \quad (4)$$

<sup>4</sup>These are distinct from the alignment prototype  $\hat{Y}$

Note that due to the fixed trajectory length, the mean squared error is a suitable similarity measure. If the length would vary, a more sophisticated measure would be necessary [9].

Using  $\mathcal{L}$  for learning the LVQ parameters, two aspects have to be considered:

- 1) As the value for  $K$  is unknown a priori, it should in general be chosen larger than expected.
- 2) Due to the winner takes all strategy,  $\mathcal{L}_{LVQ}$  only updates prototypes that have supporting samples.

In order to achieve consistent training and quantization results under these conditions, the following sections present approaches for initialization (IV-A), regularization (IV-B) and refinement (IV-C). While the initialization and regularization primarily focus on 2), the refinement, build upon the expected results using the proposed initialization and regularization approaches, focuses on 1).

For describing these approaches, the *support of a prototype* plays an integral role. The support  $\pi(\mathcal{Z})_k$  of the aligned dataset  $\mathcal{X}^\phi$  for each prototype  $Z_k \in \mathcal{Z}$  is aggregated in

$$\pi(\mathcal{Z}) = \left\{ \sum_{i=1}^N \mathbf{1}_k(i) \mid k \in [1, |\mathcal{Z}|] \right\},$$

with

$$\mathbf{1}_k(i) = \begin{cases} 1 & \text{if } z(i) = k \\ 0 & \text{else} \end{cases}.$$
(5)

A resulting set of prototypes using the approach described in this section and following subsections, for the dataset shown in figure 1, is depicted in figure 2. It can be seen, that the prototypes cover a certain range of motion patterns: constant velocity, curvilinear motion, acceleration and deceleration.

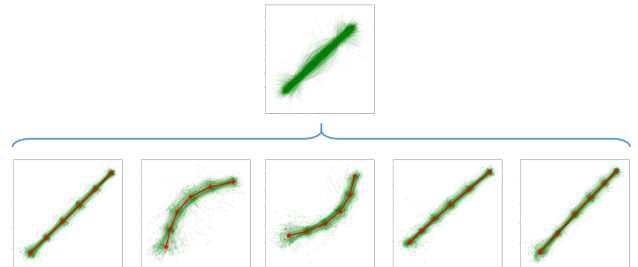


Fig. 2. Possible set of prototypes for a given dataset (top row). The prototypes represent different motion patterns (from left to right): Constant velocity, curvilinear motion, acceleration and deceleration.

##### A. Initialization

The main objective of the initialization step is two-fold. On the one hand, the number of out-of-distribution prototypes should be reduced in the initial set of prototypes  $\mathcal{Z}_{\text{init}}$ . On the other hand,  $\mathcal{Z}_{\text{init}}$  has to be spread across the data  $\mathcal{X}^\phi$ , in order to identify different motion patterns more consistently.

Taking this into account, the alignment prototype  $\hat{Y}$  is set as the first prototype  $Z_1$ , as it should resemble the most dominant motion pattern. Under the assumption that other relevant motion patterns are dissimilar to  $\hat{Y}$ , a Forgy

initialization [10] is applied for initializing the remaining  $K - 1$  prototypes. Accordingly, remaining prototypes are randomly selected from a subset  $\mathcal{X}' \subset \mathcal{X}^\phi$ , where  $\mathcal{X}'$  contains all samples  $\mathcal{X}_i^\phi$  with  $\tau_{\text{ilow}} < d_{tr}(X_i^\phi, \hat{Y}) < \tau_{\text{ihigh}}$ . The thresholds  $\tau_{\text{ix}} = Q_{q_{\text{ix}}}(\{d_{tr}(X_i^\phi, \hat{Y}) \mid X_i^\phi \in \mathcal{X}^\phi\})$  are defined as the  $q_{\text{ix}}$ -quantiles of all sample distances with respect to  $\hat{Y}$ . An upper bound  $\tau_{\text{ihigh}}$  is employed to reduce the risk of initializing a prototype with out-of-distribution samples from  $\mathcal{X}^\phi$ . Depending on the choices for  $q_{\text{ilow}}$  and  $q_{\text{ihigh}}$ , there might not be enough samples to choose from ( $|\mathcal{X}'| < K - 1$ ). In this case,  $q_{\text{ilow}}$  can be gradually reduced until  $|\mathcal{X}'| \geq K - 1$ . An example for  $\mathcal{X}$  and  $\mathcal{X}'$  with  $q_{\text{ilow}} = 0.9$  and  $q_{\text{ihigh}} = 0.95$  is given in figure 3.

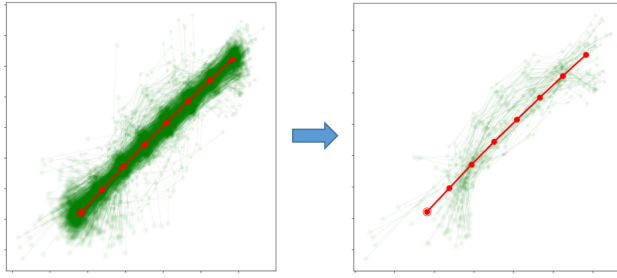


Fig. 3. Left: Aligned dataset  $\mathcal{X}^\phi$  and alignment prototype  $\hat{Y}$ . Right: Subset  $\mathcal{X}'$  for  $q_{\text{ilow}} = 0.9$  and  $q_{\text{ihigh}} = 0.95$ .

### B. Regularization

While the initialization helps in increasing the average support for each prototype<sup>5</sup>, some out-of-distribution samples<sup>6</sup> might be assigned to individual prototypes, resulting in little support from other samples.

To ensure optimization of all prototypes, a regularization term  $L_{\text{reg}}$  is employed, which is set to move out-of-distribution prototypes closer to more relevant samples or clusters of samples. Following this, different definitions for  $L_{\text{reg}}$  can be used. On the one hand,  $L_{\text{reg}}$  could move all prototypes  $Z_k \in \mathcal{Z} \setminus Z_*$  towards the most supported prototype  $Z_* = Z_{k_*}$ , where  $k_* = \arg \max_k \pi(\mathcal{Z})_k$ :

$$L_{\text{reg}} = \frac{1}{K-1} \sum_{Z_k \in \mathcal{Z} \setminus Z_*} d_{tr}(Z_k, Z_*). \quad (6)$$

Under ideal conditions,  $Z_*$  should be equal to the alignment prototype  $\hat{Y}$ , which roughly represents the overall mean of the dataset, and  $L_{\text{reg}}$  behaves accordingly. In practice, however, this assumption might not hold due to noise, increasing unpredictability of the optimization. Hence, in the following  $L_{\text{reg}}$  is defined to move all prototypes towards the global mean by minimizing the global error

$$L_{\text{reg}} = \frac{1}{N \cdot K} \sum_{i=1}^N \sum_{k=1}^K d_{tr}(X_i, Z_k). \quad (7)$$

Intuitively, by choosing an appropriate value for the regularization weight  $\gamma$ , this definition of  $L_{\text{reg}}$  moves low-support

<sup>5</sup>Compared to a simple random initialization

<sup>6</sup>Outliers or trajectories with annotation errors

prototypes in more reasonable areas within quantized space and the winner takes all loss function  $\mathcal{L}_{\text{LVQ}}$  keeps them within range of relevant sample clusters. Additionally, when  $K$  is too large, superfluous prototypes are very similar after optimization.

As a side-note, very imbalanced prototype sets, in terms of many low-support prototypes, can also be measured by the perplexity score

$$\mathcal{P}_{\mathcal{Z}} = \exp \left\{ - \sum_{k=1}^K \pi_{\text{norm}}(\mathcal{Z})_k \odot \log \{ \pi_{\text{norm}}(\mathcal{Z})_k \} \right\},$$

with

$$\pi_{\text{norm}}(\mathcal{Z})_k = \frac{\pi(\mathcal{Z})_k}{\sum_{k=1}^K \pi(\mathcal{Z})_k}. \quad (8)$$

Due to  $\mathcal{P}_{\mathcal{Z}}$  not being directly derived from  $\mathcal{Z}$ , it is not a good term for optimization, and thus for  $L_{\text{reg}}$ . Nevertheless,  $\mathcal{P}_{\mathcal{Z}}$  can be used later on when assessing the complexity of a dataset.

### C. Refinement

Finally, a heuristic refinement scheme, building on the expected results when using the regularization approach presented in section IV-C, is employed in order to remove unnecessary prototypes when  $K$  was too large. The refinement step consists of two phases. In the first phase, low-support prototypes are removed from  $\mathcal{Z}$  by using a dataset-dependent threshold  $\tau_{\text{phase1}} = \lceil \epsilon_{\text{phase1}} \cdot |X| \rceil$ :

$$\mathcal{Z}' = \mathcal{Z} \setminus \{Z_k \mid \pi(\mathcal{Z})_k < \tau_{\text{phase1}}\}. \quad (9)$$

The second phase revolves around removing prototypes similar to the most supported prototype  $Z_*$ . It is assumed, that  $Z_*$  is close to the global mean of the dataset. This implies, that superfluous prototypes are driven towards  $Z_*$  because of the global mean regularization, allowing to detect and remove these prototypes. For assessing similarity, prototypes  $Z_k \in \mathcal{Z} \setminus \{Z_*\}$  are first aligned with  $Z_*$  in terms of their starting points  $\mathbf{z}_1^k = \mathbf{z}_1^*$  and initial orientations  $\mathbf{z}_2^k - \mathbf{z}_1^k = \mathbf{z}_2^* - \mathbf{z}_1^*$ . An aligned prototype  $Z'_k$  is then considered as similar to  $Z_*$  when at least  $\epsilon_{\text{phase2}} \cdot 100\%$  of its points are in close proximity to respective points of  $Z_*$ :

$$\text{sim}(Z'_k, Z_*) = \begin{cases} \text{true} & \text{if } |\mathcal{S}(Z'_k, Z_*)| \geq \epsilon_{\text{phase2}} \cdot |Z_*| \\ \text{false} & \text{else} \end{cases},$$

with

$$\begin{aligned} \mathcal{S}(Z'_k, Z_*) &= \{ \mathbf{z}_j^k \mid \|\mathbf{z}_j^k - \mathbf{z}_j^*\|_2 < \tau(Z_*)_j, j \in [1, M] \} \\ \tau(Z_*)_j &= Q_{0.99}(\{ \|\mathbf{z}_j^* - \mathbf{x}_j\|_2 \mid \mathbf{x}_j^i \in X_i, X_i \in \mathcal{X}^\phi \}). \end{aligned} \quad (10)$$

$\tau(Z_*)_j$  is the per-point distance threshold of the  $j$ 'th trajectory point calculated from the supporting samples  $\{X_i \in \mathcal{X}^\phi \mid z(i) = k_*\}$  of  $Z_*$ . The 0.99-quantile is used instead of the maximum to exclude outliers in the data. A visual example for determining similarity is given in figure 4.

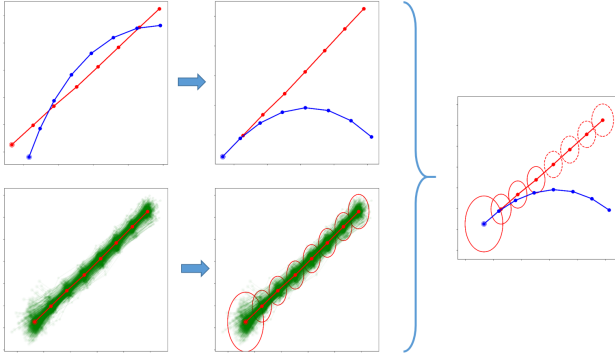


Fig. 4. Example of assessing prototype similarity in the second phase of the refinement scheme. The first row shows the alignment of a prototype  $Z_k$  (blue) with the highest-support prototype  $Z_*$  (red). The second row shows how the maximum distance per-point is estimated for determining similarity. In this example, as seen on the right,  $Z_k$  is only within similarity range for 4 of 8 points, thus it is determined as dissimilar when choosing an overlap factor  $\epsilon_{\text{phase2}} > 0.5$ .

## V. QUANTIFYING TRAJECTORY DATASET COMPLEXITY

This section discusses a first attempt in quantifying the complexity of human trajectory prediction benchmarking datasets. While previous work (e.g. [6], [11], [12]) focuses on statistics directly derived from the dataset, like for example histograms or the deviation from linear predictions, the approach proposed in the following primarily relies on the dataset representation learned by the LVQ, i.e. the set of prototypes  $\mathcal{Z}$  *after* refinement. Thus, a list of factors, expected to contribute to the complexity of a dataset, is collected. Additionally, a mathematical representation of these factors is built using  $\mathcal{Z}$  and the aligned dataset  $\mathcal{X}^\phi$ .

The first factor is given by the *number of distinct motion patterns present in the data*. This is the most obvious factor, as an increased number of motion patterns directly implies that a statistical model needs to have higher capacity in order to capture all patterns. The number of motion patterns at a given sequence length is given by the number  $K = |\mathcal{Z}|$  of prototypes representing  $\mathcal{X}^\phi$ .

The second factor targets the *diversity between motion patterns*, i.e. different motion patterns are clearly distinguishable or overlapping. In case of distinguishable patterns, a model of the data needs to be able to represent multiple modes in the data without mixing them up, again requiring higher modeling capacity. Thus, a higher diversity between motion patterns is expected to correspond to a higher dataset complexity. One possibility to measure this diversity is to use the mean pair-wise distance between the most supported prototype  $Z_*$  and all other prototypes  $Z_k \in \mathcal{Z} \setminus \{Z_*\}$ :

$$d_{\mathcal{Z}} = \frac{1}{K-1} \sum_{k \neq k_*} \frac{1}{M} d_{tr}(s_* \cdot Z_*, s_* \cdot Z'_k). \quad (11)$$

Similar to the approach for assessing the similarity between prototypes described in section IV-C, each prototype  $Z_k$  is aligned with  $Z_*$  in terms of their starting points and initial orientations, yielding  $Z'_k$ . The scaling factor  $s_* = \|\mathbf{z}_2^* - \mathbf{z}_1^*\|$  is employed to ensure comparability between datasets.

The third factor targets the *diversity between trajectories assigned to one prototype*, i.e. variations of the same pattern. A higher variation implies a higher uncertainty when modeling specific motion patterns, making it harder to capture by using statistical models. The variation, in the following denoted as the spread  $\text{spr}_{\mathcal{X}}$ , can be measured per prototype  $Z_k \in \mathcal{Z}$  by involving respective (scaled) supporting samples  $\mathcal{X}_k = \{s_* \cdot X_i \mid X_i \in \mathcal{X}^\phi, z(i) = k\}$ . Following this, the spread is calculated as the mean per-point standard deviation, separated by dimension:

$$\text{spr}_{\mathcal{X}} = \frac{1}{K} \sum_{k=1}^K \frac{1}{|\mathcal{X}_k|} s(\mathcal{X}_k),$$

with

$$s(\mathcal{X}_k) = \frac{1}{2} \sum_{d=1}^2 \frac{1}{M} \sum_{j=1}^M \sqrt{\frac{1}{N} \sum_{i=1}^{|\mathcal{X}_k|} \left( \mathbf{x}_{j,d}^i - m_d(\mathcal{X}_k) \right)^2} \\ m_{j,d}(\mathcal{X}_k) = \frac{1}{N} \sum_{i=1}^{|\mathcal{X}_k|} \mathbf{x}_{j,d}^i. \quad (12)$$

Here,  $\mathbf{x}_{j,d}^i \in X_i$  denotes the  $d$ 'th dimension ( $x$  or  $y$  position) of the  $j$ 'th trajectory point of the  $i$ 'th sample  $X_i \in \mathcal{X}_k$ .

Lastly, the *statistical relevance* or rather the *relevance distribution* of each identified motion pattern is considered. This mainly focuses on biases in the data, and thus answers the question if there is a prevalent motion pattern or if the occurrence of all patterns is equally likely. In the scope of this paper, less biased datasets are considered as more complex, because less biased data enables statistical models to capture different patterns in the first place. The relevance distribution can be quantified using the perplexity  $\mathcal{P}_{\mathcal{Z}}$  (see equation 8). As the value range of  $\mathcal{P}_{\mathcal{Z}}$  scales with  $K$ , the re-scaled perplexity

$$\mathcal{P}_{\mathcal{Z}}^r = \frac{\mathcal{P}_{\mathcal{Z}} - 1}{K - 1}, \quad (13)$$

with value range  $[0, 1]$ , is preferred.  $\mathcal{P}_{\mathcal{Z}}^r = 1$  implies that each  $Z_k \in \mathcal{Z}$  is supported equally given  $\mathcal{X}^\phi$ , while  $\mathcal{P}_{\mathcal{Z}}^r \rightarrow 0$  implies a strong bias towards a single prototype.

Finally, the four factors are combined into a single complexity score<sup>7</sup>

$$\mathcal{C} = [K] + c_1 \cdot d_{\mathcal{Z}}' + c_1 \cdot \mathcal{P}_{\mathcal{Z}}^r + c_2 \cdot \text{spr}_{\mathcal{X}}',$$

with

$$c_1 = \frac{e^1}{e^1 + e^1 + e^{\frac{1}{2}}} \\ c_2 = \frac{e^{\frac{1}{2}}}{e^1 + e^1 + e^{\frac{1}{2}}}, \quad (14)$$

trying to quantify the complexity of a given dataset and enabling a relative ordering in a multi-dataset comparison. With this definition, most emphasize is put on the number  $K$  of identified motion patterns, while the secondary factors,

<sup>7</sup> $\lfloor \cdot \rfloor$  denotes the function rounding a real number to the nearest natural number.

$d_{\mathcal{Z}}$ ,  $\mathcal{P}_{\mathcal{Z}}^r$  and  $\text{spr}_{\mathcal{X}}$ , are used for fine-tuning the complexity ranking. The relative importance of factors is ensured by normalizing and weighting the secondary factors and the fact, that  $K$  is generally  $\geq 1$ . The secondary factors are normalized to values in  $[0, 1]$  by dividing by the respective maximum values across all datasets in comparison, yielding  $d'_{\mathcal{Z}}$ ,  $\mathcal{P}'_{\mathcal{Z}}^r$  and  $\text{spr}'_{\mathcal{X}}$ . This normalization also provides more stable complexity values. Further,  $d_{\mathcal{Z}}$  and  $\mathcal{P}_{\mathcal{Z}}^r$  are weighted higher than  $\text{spr}_{\mathcal{X}}$ , attributing higher impact to factors directly derived from the prototypes. Besides that, giving  $\text{spr}_{\mathcal{X}}$  less importance is also motivated by the fact that potential noise and outliers in the support sets  $\mathcal{X}_k$  might distort the results. In addition to normalizing the individual values, the weights are set to satisfy  $2*c_1 + c_2 = 1$ , by scaling the weights using a *softmax* function.

As a final note, due to the comparison of different datasets with independently trained LVQs, the scale of resulting prototypes and aligned data might differ, thus comparability has to be ensured. In order to cope with this, the secondary complexity factors are normalized and samples, as well as prototypes, are scaled when calculating the factors. For scaling, the most supported prototype  $Z_*$  for each dataset is scaled such that  $\|\mathbf{x}_2^* - \mathbf{x}_1^*\|_2 = 1$ . The obtained scaling factor  $s_*$  is then applied to scale the respective aligned datasets and the other prototypes. Further, the same refinement parameters have to be used for all datasets in order to achieve comparable results.

## VI. EVALUATION

This section primarily focuses on a thorough complexity analysis of standard benchmarking datasets for long-term human trajectory prediction. An evaluation (section VI-A) is conducted on scenes of the following standard benchmarking datasets: BIWI Walking Pedestrians ([13], abbrev.: *biwi*), Crowds by example (also known as the UCY dataset, [14], abbrev.: *crowds*) and the Stanford Drone Dataset ([6], abbrev.: *sdd*). The scenes in the datasets are denoted as *Dataset: Scene Recording*, e.g. recording 01 of the *zara* scene in the *crowds* dataset is denoted as *crowds: zara01*. Note that for *sdd*, different recordings of the same scene do not necessarily capture the same campus area (but there might be some overlap). The section closes with a brief discussion of the results and interesting findings (section VI-B).

### A. Quantifying Benchmarking Dataset Complexity

For creating a complexity ranking of the (scene) datasets in comparison, a prototype-based dataset representation is generated for all datasets and the complexity quantification approach presented in section V is applied. In order to achieve reasonable results using a lot of different datasets, developed under different conditions in terms of recording and annotation, several setup steps are performed as explained next.

1) *Setup*: As a first step, the datasets are augmented to have a common annotation rate. The *biwi* and *crowds* scenes already have the same annotation rate of 2.5 annotations

per second, thus the annotation rate of all the *sdd* scenes is adjusted accordingly.

Next, as the prototype-based representation only works with trajectories of the same length, an appropriate sequence length has to be chosen for each dataset in the evaluation. The most commonly used sequence length in recent benchmarks is  $M = 20$  (8 for observation and 12 for predicting) points per trajectory. Setting  $M = 20$  for all datasets might, however, lead to smaller datasets having only a few trajectories left for learning the LVQ, as the average trajectory length varies greatly between datasets. Because of this, the  $q$ -quantile of trajectory lengths per dataset is chosen, i.e. a common but dataset-dependent sequence length. After choosing  $M$ , the training datasets are assembled by collecting all possible (sub-)trajectories with length  $M$  from each respective dataset, in order to provide as much data as possible. Additionally, in order to achieve a more meaningful result, the average of multiple sequence lengths, i.e. time scales, is used for calculating the complexity scores. Thus,  $q = 0.1$  and  $q = 0.25$  are used for evaluation, ensuring that a greater portion of the dataset remains, while removing less interesting trajectories in terms of long-term trajectory prediction.

Then, trajectories not exceeding a dataset-dependent minimum speed<sup>8</sup>  $s_{\min}$  are filtered. The reason for this is twofold. First, statistical models are worse in modeling trajectories of slow-moving persons, as their behavior becomes less predictable [15]. Second, and as a consequence, these trajectories generally do not contain viable motion patterns to extract. For this evaluation, the minimum speed is calculated heuristically for a given training dataset  $\mathcal{X}$  containing all possible (sub-)trajectories of length  $M$ :

$$s_{\min} = \frac{\max_i m_{\text{speed}}(i) - \min_i m_{\text{speed}}(i)}{M}$$

with

$$m_{\text{speed}}(i) = \frac{1}{M-1} \sum_{j=2}^M \|\mathbf{x}_j^i - \mathbf{x}_{j-1}^i\|_2 \quad (15)$$

Here,  $m_{\text{speed}}(i)$  denotes the average speed of the  $i$ 'th trajectory  $X_i \in \mathcal{X}$ .

Finally, for each dataset and sequence length, the training of the alignment and LVQ networks, as well as the complexity factor calculations are run 10 times. The complexity scores are then calculated on the average of these factors, in order to obtain a more robust result. The number of initial prototypes is set to  $K = 10$  for all datasets.

2) *Results*: The average results and the determined complexity scores are listed in table I. Some scenes were filtered out after the setup, as their number of samples did not exceed 150, leading to less stable alignment and LVQ models. It can be seen that the *biwi* scenes are among the least complex datasets, while the most complex scenes are found in the *sdd* dataset. For demonstration purposes, the datasets and prototypes for *biwi: eth* and *sdd: nexus11* are illustrated

<sup>8</sup>The average distance between subsequent trajectory points.

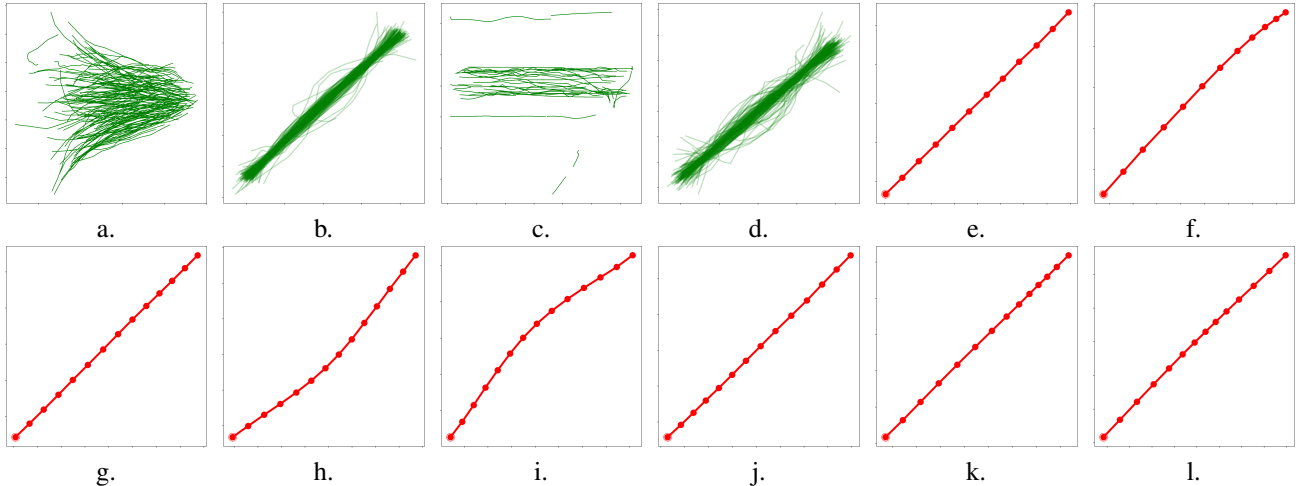


Fig. 5. Data and aligned data (a. & b.: *biwi: eth*, c. & d.: *sdd: nexus11*) with similar sequence lengths (12 & 14), as well as learned prototypes for *biwi: eth* (e. & f.) and *sdd: nexus11* (g. – l.). Having a higher complexity score, *sdd: nexus11* consists of a higher variety of motion patterns, including constant velocity (g.), curvilinear motion (h. & i.), acceleration (j.), deceleration (k.) and a mixed pattern (l.). The fraction of samples assigned to each prototype are 93% (a.) and 7% (b.) for *biwi: eth* and 43.5% (g.), 19.4% (h.), 13.7% (i.), 8.6% (j.), 5.6% (k.) and 9.2% (l.) for *sdd: nexus11*.

in figure 5 for similar sequence lengths (12 and 14). As opposed to *biwi: eth*, *sdd: nexus11*, being the dataset with the highest complexity score, consists of thrice the amount of motion patterns, including constant velocity, curvilinear motion, acceleration and deceleration, as well as a mixed motion pattern. This mixed pattern consists of constant velocity, decelerating and accelerating parts, and might occur due to the rather high sequence length with respect to the covered time span.

### B. Discussion

An interesting case is given by the *crowds* scenes *zara01* and *zara02* (and *zara03*, but this scene is often left out in state-of-the-art comparisons). Although these scenes were recorded with the same camera from the same angle and were annotated under the same conditions, their complexity scores, as well as some of the complexity factors vary quite significantly. On the one hand, the higher ranking of *zara01* can be confirmed by different state-of-the-art models (e.g. [16], [17], [18]) by achieving slightly better results on *zara02*. On the other hand, *zara02* shows high intra-pattern diversity in the data for  $M = 23$ , which could be an indicator that statistical models are well capable of handling intra-pattern variations.

Further, all datasets in this comparison are recorded from a birds-eye view. Because of that it could be expected, that there are common motion patterns in all datasets, independent of the time horizon. This fact has been, with a few exceptions, confirmed, in that almost all scenes contain slight variations of the basic motion patterns: constant velocity, acceleration and deceleration, as well as curvilinear motion. Some datasets contain multiple variations of the same basic motion pattern or even mixed motion patterns, enabled by the, partially, high sequence length  $M$ . This can, for example, be seen in figure 5 (g. – l.).

Lastly, another aspect related to the motion patterns found in the data is, that in all datasets, the constant velocity

pattern is the dominant, i.e. most supported, motion pattern, covering a large fraction of the entire dataset (see figure 6 for exemplary fractions for low to high complexity scene datasets). This has multiple implications related to common evaluation methodology in current state-of-the-art publications. On the one hand, it is a perfect explanation for the difficulties in beating a simple linear extrapolation model in the task of human trajectory prediction. This phenomenon could for example be observed during the TrajNet challenge [1], where multiple of the first submissions failed to beat the linear model. On the other hand, this fact indicates, that an arbitrarily assembled benchmarking data basis poses the risk of rendering corner cases, i.e. motion patterns different from the constant velocity pattern, statistically irrelevant. This leads to statistical models that are incapable of modeling more complex motion, that might also struggle with beating a linear model.

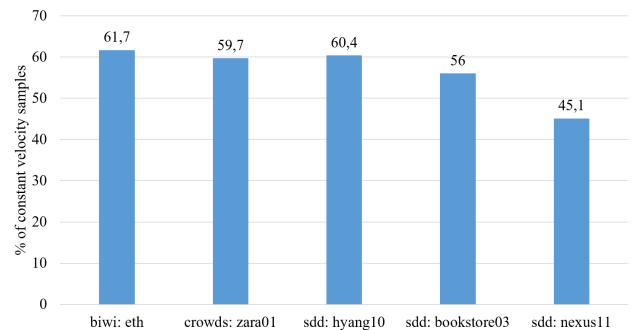


Fig. 6. Depicts the fraction of samples assigned to the constant velocity prototype (sample ratio) for a range of low to high complexity scene datasets. The fractions are calculated by taking the mean sample ratio, taking all iterations and sequence lengths considered in table I into account. Even with a high number of distinct motion patterns in the data (e.g. *sdd: nexus11*), constant velocity samples make up 45% of all samples in the dataset.

Dataset	$\mathcal{C}$	Sequence Length ( $M$ )									
		0.1-quantile				0.25-quantile					
		$ \mathcal{X}  (M)$	$ \mathcal{Z} $	$d_{\mathcal{Z}}$	$\mathcal{P}_{\mathcal{Z}}^r$	$spr_{\mathcal{X}}$	$ \mathcal{X}  (M)$	$ \mathcal{Z} $	$d_{\mathcal{Z}}$	$\mathcal{P}_{\mathcal{Z}}^r$	$spr_{\mathcal{X}}$
sdd: hyang13	3.311	453 (4)	2.4	0.144	0.621	0.075	481 (6)	3.5	0.301	0.770	0.110
sdd: hyang14	3.412	389 (9)	4.4	1.146	0.793	0.295	188 (26)	2.0	4.819	0.323	1.062
crowds: zara03	3.464	2199 (17)	2.3	1.668	0.652	0.650	999 (27)	3.8	4.837	0.598	1.426
<b>biwi: eth</b>	<b>3.822</b>	<b>2412 (9)</b>	<b>4.7</b>	<b>0.387</b>	<b>0.870</b>	<b>0.103</b>	<b>1534 (12)</b>	<b>2.3</b>	<b>0.683</b>	<b>0.489</b>	<b>0.225</b>
biwi: hotel	3.848	3155 (6)	4.3	0.271	0.761	0.097	2151 (10)	2.9	0.431	0.770	0.134
sdd: hyang05	3.894	4460 (21)	4.0	3.007	0.426	0.959	3333 (29)	2.8	3.262	0.523	1.209
sdd: deathCircle02	3.986	244 (12)	3.4	1.220	0.852	0.484	164 (16)	3.9	3.405	0.785	0.727
sdd: nexus00	4.020	3668 (28)	4.3	2.378	0.820	0.900	2607 (42)	3.5	4.671	0.614	1.392
sdd: bookstore00	4.040	5359 (16)	3.7	1.434	0.785	0.502	3856 (27)	3.3	6.621	0.597	2.171
<b>crowds: zara02</b>	<b>4.096</b>	<b>2305 (23)</b>	<b>4.4</b>	<b>2.949</b>	<b>0.663</b>	<b>9.461</b>	<b>1387 (28)</b>	<b>3.1</b>	<b>4.532</b>	<b>0.588</b>	<b>1.224</b>
sdd: nexus04	4.369	374 (4)	4.1	0.183	0.592	0.101	912 (15)	4.1	1.623	0.876	0.559
sdd: coupa00	4.408	2040 (11)	4.7	0.795	0.790	0.238	1459 (24)	2.8	3.061	0.580	0.920
sdd: coupa03	4.445	2534 (14)	5.3	0.935	0.762	0.255	1842 (30)	2.8	2.805	0.792	0.993
sdd: hyang01	4.508	5246 (19)	5.3	1.440	0.820	0.446	3661 (37)	3.1	7.271	0.388	1.209
<b>crowds: zara01</b>	<b>4.521</b>	<b>1686 (24)</b>	<b>3.6</b>	<b>2.825</b>	<b>0.690</b>	<b>0.989</b>	<b>1139 (28)</b>	<b>4.2</b>	<b>4.153</b>	<b>0.763</b>	<b>1.229</b>
sdd: nexus02	4.848	4892 (6)	5.1	0.395	0.715	0.183	3762 (21)	3.9	1.810	0.604	0.502
sdd: gates02	4.866	1521 (11)	5.3	0.769	0.745	0.181	1276 (14)	3.8	1.355	0.677	0.337
sdd: nexus09	4.874	2797 (6)	4.1	0.347	0.600	0.158	2518 (27)	5.5	3.012	0.683	0.791
sdd: gates07	4.896	460 (9)	3.8	0.834	0.775	0.229	348 (15)	4.9	1.665	0.735	0.381
sdd: nexus10	4.903	1948 (12)	4.9	0.633	0.839	0.230	1550 (22)	3.9	1.570	0.734	0.510
sdd: deathCircle01	4.917	15941 (9)	5.4	0.781	0.754	0.268	10458 (18)	4.0	2.595	0.724	0.808
sdd: little03	4.921	5510 (15)	5.2	1.659	0.796	0.456	4392 (21)	4.5	2.488	0.588	0.885
sdd: gates05	4.938	999 (6)	5.2	0.482	0.870	0.201	697 (14)	3.8	1.993	0.839	0.431
sdd: hyang02	4.957	5599 (19)	5.3	2.401	0.697	0.750	4038 (27)	3.9	3.736	0.580	1.079
sdd: hyang03	4.963	4814 (15)	5.2	1.410	0.789	0.486	3916 (23)	3.8	3.392	0.705	0.917
sdd: little01	5.296	1874 (10)	5.1	0.540	0.632	0.178	1475 (14)	4.8	0.973	0.546	0.258
sdd: coupa01	5.331	2043 (6)	6.3	0.253	0.769	0.121	1966 (19)	4.0	1.308	0.557	0.430
sdd: gates00	5.366	2072 (14)	5.6	0.580	0.762	0.186	1550 (20)	4.2	1.141	0.713	0.334
<b>sdd: hyang10</b>	<b>5.395</b>	<b>1496 (16)</b>	<b>4.9</b>	<b>1.723</b>	<b>0.601</b>	<b>0.397</b>	<b>1315 (20)</b>	<b>4.9</b>	<b>2.541</b>	<b>0.676</b>	<b>0.475</b>
sdd: deathCircle04	5.404	449 (7)	5.9	1.168	0.757	0.292	363 (9)	4.3	1.137	0.814	0.361
sdd: bookstore06	5.418	1810 (10)	5.4	0.752	0.827	0.220	1355 (18)	4.8	2.621	0.674	0.509
sdd: little00	5.426	734 (15)	6.5	1.803	0.725	0.346	521 (20)	4.5	1.939	0.767	0.422
sdd: nexus01	5.428	7825 (15)	5.7	0.887	0.834	0.368	6022 (32)	4.2	3.584	0.543	0.928
sdd: gates01	5.503	5419 (14)	4.8	1.947	0.826	0.426	3814 (22)	5.4	3.412	0.806	0.673
sdd: coupa02	5.848	2380 (8)	5.5	0.466	0.666	0.186	2075 (16)	5.0	0.932	0.766	0.299
sdd: bookstore05	5.851	2217 (6)	4.6	0.307	0.763	0.161	2075 (10)	5.6	0.661	0.741	0.194
sdd: bookstore04	5.853	592 (4)	4.8	0.119	0.732	0.053	1906 (15)	5.9	1.194	0.735	0.362
sdd: nexus08	5.872	3168 (11)	5.5	0.497	0.772	0.179	2664 (21)	5.1	1.007	0.754	0.353
sdd: bookstore01	5.874	3103 (6)	5.6	0.292	0.763	0.131	4488 (13)	5.0	0.802	0.833	0.248
<b>sdd: bookstore03</b>	<b>5.877</b>	<b>5698 (9)</b>	<b>6.0</b>	<b>0.458</b>	<b>0.838</b>	<b>0.128</b>	<b>4054 (20)</b>	<b>5.1</b>	<b>2.175</b>	<b>0.574</b>	<b>0.434</b>
sdd: hyang11	5.884	3347 (12)	5.6	0.810	0.731	0.236	2746 (21)	4.7	1.856	0.696	0.508
sdd: nexus06	5.896	3633 (16)	5.6	0.894	0.742	0.337	2906 (30)	4.6	2.906	0.588	0.670
sdd: gates08	5.921	736 (10)	5.7	0.721	0.846	0.220	563 (17)	4.7	1.558	0.811	0.430
sdd: nexus07	5.933	4162 (16)	5.3	1.062	0.798	0.332	3419 (26)	5.5	2.746	0.710	0.568
sdd: hyang06	5.941	4114 (16)	6.1	1.667	0.676	0.439	3027 (31)	5.1	4.762	0.514	1.014
sdd: gates04	5.951	1632 (8)	5.5	0.664	0.847	0.232	1146 (19)	5.3	2.305	0.854	0.548
sdd: deathCircle00	5.987	16682 (12)	6.2	1.288	0.811	0.318	10720 (26)	4.7	3.939	0.745	1.044
sdd: gates03	5.989	8237 (11)	5.8	1.200	0.875	0.293	5645 (20)	4.9	3.381	0.798	0.627
sdd: hyang04	6.038	14771 (18)	5.2	2.264	0.700	0.547	10288 (36)	5.6	6.859	0.580	1.403
sdd: nexus03	6.114	1035 (10)	4.9	2.198	0.761	0.559	854 (22)	6.5	6.275	0.798	4.147
sdd: gates06	6.349	223 (5)	5.8	0.326	0.743	0.111	213 (6)	5.6	0.388	0.792	0.083
sdd: hyang12	6.358	1660 (12)	5.0	0.619	0.695	0.186	1371 (19)	6.9	1.267	0.722	0.292
sdd: bookstore02	6.448	6571 (11)	6.6	1.009	0.817	0.247	4782 (22)	5.2	3.039	0.736	0.538
sdd: hyang00	6.538	10976 (19)	6.2	1.903	0.810	4.891	6172 (29)	5.8	3.564	0.708	0.774
sdd: little02	6.826	941 (10)	6.5	0.490	0.629	0.125	728 (13)	7.4	0.596	0.750	0.157
sdd: hyang07	6.920	497 (7)	5.7	0.439	0.710	0.131	355 (20)	7.4	2.298	0.899	0.286
<b>sdd: nexus11</b>	<b>7.388</b>	<b>2012 (14)</b>	<b>6.6</b>	<b>0.725</b>	<b>0.763</b>	<b>0.235</b>	<b>1867 (23)</b>	<b>7.2</b>	<b>0.958</b>	<b>0.812</b>	<b>0.356</b>

TABLE I

COMPLEXITY SCORES, CHOSEN SEQUENCE LENGTHS AND AVERAGE COMPLEXITY FACTORS FOR SCENE DATASETS IN COMPARISON ORDERED BY COMPLEXITY. SCENE DATASETS REFERRED TO IN THE RESULTS AND DISCUSSION SECTIONS ARE HIGHLIGHTED.

## VII. CONCLUSIONS

This paper proposed an approach for generating a quantized representation of trajectory datasets, relying on an alignment followed by vector quantization. Building on this representation, an approach for calculating different complexity factors and an aggregated relative complexity score have been presented. Using these factors and the score, commonly used benchmarking datasets for human trajectory prediction have been ranked, showing that the *biwi* dataset scenes are among the least complex scenes and the most complex scenes are found in the *sdd* dataset. The complexity ranking was followed by a brief discussion on indications for human trajectory prediction and benchmarking, stressing the importance of a well-rounded data basis. In addition, it touched on common characteristics and variance in birds-eye view datasets.

## REFERENCES

- [1] A. Sadeghian, V. Kosaraju, A. Gupta, S. Savarese, and A. Alahi, “Trajnet: Towards a benchmark for human trajectory prediction,” *arXiv preprint*, 2018.
- [2] A. Rudenko, L. Palmieri, M. Herman, K. M. Kitani, D. M. Gavrila, and K. O. Arras, “Human motion trajectory prediction: A survey,” *arXiv preprint arXiv:1905.06113*, 2019.
- [3] L. v. d. Maaten and G. Hinton, “Visualizing data using t-sne,” *Journal of machine learning research*, vol. 9, no. Nov, pp. 2579–2605, 2008.
- [4] I. T. Jolliffe and J. Cadima, “Principal component analysis: a review and recent developments,” *Philosophical Transactions of the Royal Society A: Mathematical, Physical and Engineering Sciences*, vol. 374, no. 2065, p. 20150202, 2016.
- [5] R. Hug, S. Becker, W. Hübner, and M. Arens, “A short note on analyzing sequence complexity in trajectory prediction benchmarks,” *2nd Workshop on Long-term Human Motion Prediction*, 2020.
- [6] A. Robicquet, A. Sadeghian, A. Alahi, and S. Savarese, “Learning social etiquette: Human trajectory understanding in crowded scenes,” in *European conference on computer vision*. Springer, 2016, pp. 549–565.
- [7] T. Kohonen, M. R. Schroeder, and T. S. Huang, *Self-Organizing Maps*, 3rd ed. Berlin, Heidelberg: Springer-Verlag, 2001.
- [8] A. van den Oord, O. Vinyals, *et al.*, “Neural discrete representation learning,” in *Advances in Neural Information Processing Systems*, 2017, pp. 6306–6315.
- [9] J. Quehl, H. Hu, Ö. S. Taş, E. Rehder, and M. Lauer, “How good is my prediction? finding a similarity measure for trajectory prediction evaluation,” in *2017 IEEE 20th International Conference on Intelligent Transportation Systems (ITSC)*. IEEE, 2017, pp. 1–6.
- [10] J. M. Pena, J. A. Lozano, and P. Larrañaga, “An empirical comparison of four initialization methods for the k-means algorithm,” *Pattern recognition letters*, vol. 20, no. 10, pp. 1027–1040, 1999.
- [11] R. Hug, S. Becker, W. Hübner, and M. Arens, “On the reliability of lstm-mdl models for pedestrian trajectory prediction,” *VIIth International Workshop on Representation, analysis and recognition of shape and motion From Image data (RFMI 2017)*, 2017.
- [12] S. Becker, R. Hug, W. Hübner, and M. Arens, “Red: A simple but effective baseline predictor for the trajnet benchmark,” in *The European Conference on Computer Vision (ECCV) Workshops*, September 2018.
- [13] S. Pellegrini, A. Ess, K. Schindler, and L. van Gool, “You’ll never walk alone: Modeling social behavior for multi-target tracking,” in *International Conference on Computer Vision*, 2009, pp. 261–268.
- [14] A. Lerner, Y. Chrysanthou, and D. Lischinski, “Crowds by example,” *Computer Graphic Forum*, vol. 26, no. 3, pp. 655–664, 2007. [Online]. Available: <http://dblp.uni-trier.de/db/journals/cgf/cgf26.html#LernerCL07>
- [15] I. Hasan, F. Setti, T. Tsesmelis, V. Belagiannis, S. Amin, A. Del Bue, M. Cristani, and F. Galasso, “Forecasting people trajectories and head poses by jointly reasoning on tracklets and vislets,” *IEEE Transactions on Pattern Analysis and Machine Intelligence*, pp. 1–1, 2019.
- [16] A. Alahi, K. Goel, V. Ramanathan, A. Robicquet, L. Fei-Fei, and S. Savarese, “Social lstm: Human trajectory prediction in crowded spaces,” in *The IEEE Conference on Computer Vision and Pattern Recognition (CVPR)*, June 2016.
- [17] I. Hasan, F. Setti, T. Tsesmelis, A. Del Bue, F. Galasso, and M. Cristani, “Mx-lstm: Mixing tracklets and vislets to jointly forecast trajectories and head poses,” in *The IEEE Conference on Computer Vision and Pattern Recognition (CVPR)*, June 2018.
- [18] P. Zhang, W. Ouyang, P. Zhang, J. Xue, and N. Zheng, “Sr-lstm: State refinement for lstm towards pedestrian trajectory prediction,” in *The IEEE Conference on Computer Vision and Pattern Recognition (CVPR)*, June 2019.